ELSEVIER

Expression of prestin, a membrane motor protein, in the mammalian auditory and vestibular periphery

Henry J. Adler *, Inna A. Belyantseva, Raymond C. Merritt Jr., Gregory I. Frolenkov, Gerard W. Dougherty, Bechara Kachar

Section on Structural Cell Biology, National Institute on Deafness and Other Communication Disorders, National Institutes of Health, Bldg. 50, Room 4249, Bethesda, MD 20892-8027, USA

Abstract

Hair cells are specialized mechanoreceptors common to auditory and vestibular sensory organs of mammalian and non-mammalian species. Different hair cells are believed to share common features related to their mechanosensory function. It has been shown that hair cells possess various forms of motile properties that enhance their receptor function. Membrane-based electromotility is a form of hair cell motility observed in isolated outer hair cells (OHCs) of the cochlea. A novel membrane protein, prestin, recently cloned from gerbil and rat tissues, is presumably responsible for electromotility. We cloned prestin from mouse organ of Corti and confirmed strong homology of this protein among different rodent species. We explored whether or not prestin is present in hair cells of the vestibular system. Using reverse transcription-polymerase chain reaction, we demonstrated that prestin is expressed in mouse and rat auditory and vestibular organs, but not in chicken auditory periphery. *In situ* hybridization and immunolocalization studies confirmed the presence of prestin in OHCs as well as in vestibular hair cells (VHCs) of rodent saccule, utricle and crista ampullaris. However, in the VHCs, staining of varying intensity with anti-prestin antibodies was observed in the cytoplasm, but not in the lateral plasma membrane or in the stereociliary membrane. Whole-cell patch-clamp recordings showed that VHCs do not possess the voltage-dependent capacitance associated with membrane-based electromotility. We conclude that although prestin is expressed in VHCs, it is unlikely that it supports the form of somatic motility observed in OHCs.
© 2003 Elsevier B.V. All rights reserved.

Key words: Sensory transduction; Hair cell; Electromotility

1. Introduction

Hair cells, specialized sensory cells that use hair bundles to sense the external mechanical stimulation, are ubiquitous among vertebrates (Pickles and Corey, 1992). Among different species and organs, hair cells share many common features, including an active force-generating mechanism in the stereociliary bundle (Manley, 2000). Active movements of the hair bundles have been observed in the auditory hair cells of the turtle (Crawford and Fettiplace, 1985), in vestibular hair cells (VHCs) of the bullfrog (Denk and Webb, 1992; Benser et al., 1996), and in the VHCs of the eel (Rusch and Thurm, 1990). Evidence for such movements has been reported for auditory hair cells of lizards (Manley et al., 2001) and birds (Manley and Koppl, 1998). The force-generating mechanism in the hair bundle activates in a submillisecond time scale and is closely related to the operation of mechanosensitive transduction channels (Ricci et al., 2000). This mechanism appears strong enough to amplify sound-induced vibrations in the auditory periphery (Martin

* Corresponding author. Tel.: +1 (301) 402-1601;
Fax: +1 (301) 402-1765.
E-mail address: adlerh@nidcd.nih.gov (H.J. Adler).

Abbreviations: OHC, outer hair cell; VHC, vestibular hair cell; RT-PCR, reverse transcription-polymerase chain reaction; ORF, open reading frame; PBS, phosphate-buffered saline

and Hudspeth, 1999). The molecular components of this mechanism have not yet been identified.

In mammals, slow (Griguer et al., 1993) and fast (Zenner et al., 1992) active movements of the hair bundle and cuticular plate have been reported in VHCs. One type of hair cells in the mammalian cochlea, the outer hair cells (OHCs), have a unique ability to contract and elongate in response to changes in intracellular potential (Brownell et al., 1985; Kachar et al., 1986; Ashmore, 1987; for review see Frolenkov et al., 1998). This unique type of cell motility, known as membrane-based electromotility, operates at acoustic frequencies (Dallos and Evans, 1995; Gale and Ashmore, 1997), does not require ATP hydrolysis (Kachar et al., 1986), and is driven by voltage-dependent conformational changes of proteins embedded in the lateral plasma membrane (Kalinec et al., 1992). Prestin, a recently cloned protein containing a sulfate transporter motif, is the likely candidate for the OHC 'motor' (Zheng et al., 2000). The hypothesis that prestin is the OHC 'motor' is supported by the observation that a targeted deletion of the prestin gene causes a loss of electromotility and elevated auditory sensitivity in mice (Liberman et al., 2002). Furthermore, prestin is localized in the lateral plasma membrane of OHCs (Belyantseva et al., 2000). Its incorporation in the membrane occurs concurrently with the appearance of OHC electromotility during development of the organ of Corti in rat (Belyantseva et al., 2000). In addition, cultured human kidney cells transfected with prestin exhibit voltage-induced shape changes and voltage-dependent capacitance (Zheng et al., 2000; Santos-Sacchi et al., 2001; Ludwig et al., 2001; Meltzer and Santos-Sacchi, 2001; Santos-Sacchi and Navarrete, 2002; for review, see Dallos and Fakler, 2002; Zheng et al., 2002a), which also are characteristic of electromotility in OHCs (Santos-Sacchi, 1991).

In the organ of Corti, prestin was shown to be expressed exclusively in the OHCs but not in the inner hair cells (Belyantseva et al., 2000; Zheng et al., 2000, 2002b). However, if prestin functions as a distinct biological actuator capable of directly converting voltage to movement, then this protein may be employed by any other hair cells that require voltage-to-movement conversion at acoustic frequencies. In this study we used reverse transcription-polymerase chain reaction (RT-PCR), *in situ* hybridization, and immunofluorescence with prestin-specific probes to explore whether or not prestin is also present and similarly expressed in VHCs as in OHCs. We also attempted to determine whether prestin is expressed in hair cells of chickens, a well-studied non-mammalian species.

2. Materials and methods

2.1. RT-PCR

Adult mice (*Mus musculus*, $n = 10$), adult rats (*Rattus norvegicus*, $n = 10$), and chickens (*Gallus domesticus*, postnatal day 11, $n = 12$) were sacrificed via CO_2 overdose, and decapitated, according to the National Institutes of Health Guidelines for Animal Use. Rodent organs of Corti and vestibular tissues (saccule, utricle, and three cristae ampullares) as well as the auditory portion of the chicken inner ear (i.e., basilar papilla) were extracted and frozen on dry ice. RNA was isolated from these tissues, using the RNeasy procedure (Qiagen, Valencia, CA, USA). During the procedure, the RNA was treated with DNase I (Qiagen). Prior to reverse transcription, the RNA concentrations of rat organ of Corti, rat vestibule, mouse organ of Corti, mouse vestibule, and chicken basilar papilla were 30, 320, 96, 70, and 56 ng/µl, respectively. The RNA was reverse-transcribed into cDNA, using Superscript II (Life Technologies, Rockville, MD, USA).

The cDNA was amplified by PCR, using pairs of oligonucleotide primers (Table 1) whose design was based on the gerbil prestin open reading frame (ORF; GenBank accession number AF230376, Zheng et al., 2000). PCR products were generated using one-time activation of AmpliTaq Gold (Applied Biosystems, Foster City, CA, USA) at 94°C followed by 35–38 cycles of denaturing at 94°C for 45 s, annealing at 55°C for 45 s, and extending at 72°C for 1 min. PCR products were electrophoresed and purified via either the QIAquick PCR purification method or the QIAquick gel extraction method (Qiagen). Following ligation into the pGEM-T easy vector (Promega, Madison, WI, USA) and transformation into DH5α competent cells (Life Technologies), the PCR products were sequenced by an automated ABI 377 DNA sequencer (Applied Biosystems).

Table 1
Prestin oligonucleotide primers

Primer ID	Sequence	Nucleotide position of mouse prestin ORF
Pres7F	5′-gttgggtggcaaggagttta-3′	Nucleotides 816–835
Pres6R	5′-acagggaggacacaaaggtg-3′	Reverse complementary to nucleotides 1422–1441
Pres13F	5′-ggatcatgctgaagaaaatg-3′	Nucleotides 3–22
Pres13R	5′-cacacctccaatcatcaagc-3′	Reverse complementary to nucleotides 422–441

2.2. Cloning and sequencing of mouse prestin cDNA

Oligonucleotide primers based on the gerbil prestin DNA sequence (GenBank accession number AF230376, Zheng et al., 2000) were used to obtain numerous DNA regions from mouse organ of Corti (the shortest was 186 bp and the longest was 626 bp) via RT-PCR as described above. EditSeq and SeqMan programs (DNASTAR, Madison, WI, USA) were used to compile these sequences to form a complete ORF for mouse prestin.

2.3. Immunocytochemistry

Sprague–Dawley adult rats (Taconic, Germantown, NY, USA), C57Bl/6 adult mice (MST) and gerbils were euthanized by CO_2 and decapitated according to the NIH Guidelines for Animal Use. The bullae were removed and the cochleae were perfused through the round window with 4% paraformaldehyde in phosphate-buffered saline (PBS) and incubated in this fixative for 1 h at room temperature. The organ of Corti and vestibular tissues were dissected from the cochlear spiral in PBS using a fine needle. Samples were permeabilized in 0.5% Triton X-100 (Polysciences, Warrington, PA, USA) for 30 min and then washed in PBS. Nonspecific binding sites were blocked using 5% normal goat serum (Gibco-BRL, Gaithersburg, MD, USA) and 2% bovine serum albumin (ICN Biomedicals, Aurora, OH, USA) in PBS for 2 h. Samples were incubated for 2 h in the primary antibodies at a concentration of ∼5 μg/ml in blocking solution. After several rinses in PBS, samples were incubated in a 1:200 dilution of the fluorescein-conjugated anti-rabbit IgG secondary antibody (Amersham, Arlington Heights, IL, USA) for 40 min. In some experiments, rhodamine-phalloidin was used to visualize F-actin in stereocilia and hair cell bodies as described previously (Beyer et al., 2000). Samples were mounted using ProLong Antifade Kit (Molecular Probes, Eugene, OR, USA) and viewed with an Axiophot microscope (Carl Zeiss, Göttingen, Germany) or a 510 Laser Scanning Confocal microscope (Carl Zeiss) with a 63× objective (N.A. = 1.4).

2.4. Antibodies

To produce antibodies against prestin, rabbits were immunized with synthetic peptides corresponding to portions of the C- or N-terminal domain of the gerbil prestin [PB121, residues 725–744, SAPPPQDDMEP-NATPTTPEA; PB123, residues 15–30, KYHVER-PIFSHPVLQE, and PB129, residues 273–288, GGKEFNERFKEKLPA; GenBank accession number AF230376, Zheng et al., 2000]. Two rabbits for each

immunogenic peptide provided a high antibody titer. Antibodies were affinity-purified against corresponding peptides.

2.5. In situ hybridization

In situ hybridization of whole mounts of organ of Corti and vestibular tissues were performed based on a modification of the protocol of Braissant and Wahli (1998a,b) designed for tissue sections. Inner ear tissues were fixed overnight in 4% paraformaldehyde in DEPC-treated PBS at 4°C and dissected from the surrounding bone structures as described earlier (Morsli et al., 1998; Everett et al., 1999). Tissues were washed twice for 15 min in PBS containing 0.1% active DEPC, equilibrated in 5×SSC (NaCl 0.75 M, Na-citrate 0.075 M) for 15 min, and prehybridized for 2 h at 58°C in the hybridization mix (50% formamide, 5×SSC, salmon sperm DNA 40 μg/ml). Sense and antisense probes specific to nucleotides 816–1441 (626 bp) and nucleotides 1156–1441 (286 bp) of rat prestin ORF (GenBank accession number AJ303372, Ludwig et al., 2001) were denatured for 5 min at 80°C and added to the hybridization mix (500 ng/ml) for overnight incubation at 58°C in a humidified hybridization chamber. Following washes of increasing stringencies (30 min in 2×SSC at room temperature, 1 h in 2×SSC at 65°C, 1 h in 0.1×SSC at 65°C) and equilibration in buffer I (Tris–HCl 100 mM and NaCl 150 mM, pH 7.5), the specimens were incubated for 2 h at room temperature in buffer I containing 1:5000 alkaline phosphate-conjugated anti-digoxigenin antibody (Roche, Basel, Switzerland). After several buffer I washes, the specimens were briefly equilibrated in buffer 2 (Tris–HCl 100 mM, NaCl 100 mM, $MgCl_2$ 50 mM, pH 9.5) and subjected to overnight color development in buffer 2 containing nitroblue tetrazolium and 5-bromo-4-chloro-3-indolyl phosphate substrates (Roche). The staining reaction was stopped by a 10-min wash in Tris/EDTA (pH 8.0). After several water washes, the specimens were mounted between slide and coverslip using water-based medium (Immu-Mount, Shandon, Pittsburg, PA, USA) and examined on an Axiophot microscope (Carl Zeiss).

2.6. Hair cell isolation

Adult guinea pigs (200–400 g) were sacrificed with CO_2 and decapitated according to NIH Guidelines for Animal Use. Strips of the organ of Corti were dissected in a modified Leibowitz cell culture medium (L-15, Life Technologies) containing (in mM): NaCl (137), KCl (5.4), $CaCl_2$ (1.3), $MgCl_2$ (1.0), Na_2HPO_4 (1.0), KH_2PO_4 (0.44), $MgSO_4$ (0.81). Cristae ampullares were dissected in a modified Hanks' balanced salt solu-

tion (HBSS, Life Technologies) with high Mg^{2+} (10 mM) and low Ca^{2+} (20 μM) concentrations. The osmolarity of all solutions was adjusted to 325 ± 2 mOsm with D-glucose and the pH was adjusted to 7.35 with NaOH. To isolate hair cells, collagenase type IV (Life Technologies) was added to modified HBSS or L-15 to get a final concentration of 1 mg/ml. Preparations were incubated in the respective collagenase-containing solutions for 30 min at room temperature. After incubation, cells were dissociated by gentle reflux of the tissue through the needle of a Hamilton syringe [Model N (Cemented Needle) 705, 22 gauge] and allowed to settle on the slide for 5–10 min. Hair cells were placed in a laminar flow bath (100 μl), with exchange of solution (about 5 ml/h) by a pressurized perfusion system (BPS-4; ALA Scientific Instruments, Westbury, NY, USA), and maintained at room temperature (22–24°C) throughout the experiments.

2.7. Patch-clamp recordings and capacitance measurements

Hair cells were visualized under an inverted microscope (Axiovert 200, Carl Zeiss) equipped with differential interference contrast optics. In this study, we used only the cells without visible damage of the stereocilia and without visible dislocation of intracellular organelles. Conventional patch-clamp recordings were performed using an Axopatch 1D amplifier controlled by pClamp 7.0 software (Axon Instruments, Foster City, CA, USA). Patch-clamp pipettes were pulled from 1.0-mm o.d. borosilicate glass (#30-30-0, FHC, Bowdoinham, ME, USA) using a programmable puller (P87, Sutter Instruments, Novato, CA, USA). Pipettes were filled with a CsCl-based intracellular solution containing (in mM): CsCl (140), $MgCl_2$ (2.0), EGTA (5.0), HEPES (5), adjusted to pH 7.2 with CsOH and brought to 325 mOsm with D-glucose. The uncompensated pipette resistance was typically 3–5 MΩ when measured in the bath and the access resistance did not exceed 15 MΩ under whole-cell patch-clamp conditions. Potentials were corrected off-line for the error due to the access resistance.

Measurements of membrane capacitance were performed using the 'membrane test' feature of the pCLAMP 7.0 acquisition software as described previously (Frolenkov et al., 2000). The capacitance readings were obtained continuously at a rate of 25 Hz. To obtain the voltage dependence of the cell capacitance, the intracellular potential was forced to follow triangular voltage ramps, from -100 mV to $+160$ mV in 6 s. Measurements of the membrane capacitance during test ramps were fitted with:

$$C_m(V) = C_0 + C_{non-lin}(V) =$$

$$C_0 + 4C_{max}\frac{\exp(-(V-V_p)/W)}{[1 + \exp(-(V-V_p)/W)]^2}$$

which is the derivative of a Boltzmann function. C_0 is the linear (voltage-independent) capacitance, $C_{non-lin}$ is the non-linear (voltage-dependent) capacitance, C_{max} is the maximum voltage-dependent capacitance, V_p is the potential at the peak of $C_m(V)$, and W is a constant, which is a measure of the sensitivity of the non-linear charge displacement to potential.

3. Results

3.1. Cloning, sequencing, and characterization of mouse prestin

Prestin has already been cloned from gerbil and rat organ of Corti cDNA libraries via various means (Zheng et al., 2000; Ludwig et al., 2001). Gerbil and rat prestin have been shown to have high amino acid identity as well as sharing several structural characteristics such as the number of transmembrane domains. The purposes of cloning and characterizing mouse prestin here are to compare it with the gerbil and rat orthologs at both molecular and structural levels as well as to compare the expression of prestin in both rat and mouse organs of Corti and vestibular organs.

Multiple rounds of RT-PCR with six different pairs of oligonucleotides (including Pres7F, 6R, 13F and 13R) on mouse organ of Corti cDNA followed by ligation, transformation, and two-way sequencing yielded six DNA fragments. These fragments were compiled to form a 2.235-kb contig. BLAST searches of non-redundant nucleotide databases on this contig yielded 90% and 92% identities with the gerbil (GenBank accession number AF230376) and rat (GenBank accession number AJ303372) ORF encoding prestin, respectively. Based on these identities, the contig is the mouse prestin ORF, and was submitted as GenBank accession number AY024359. Mouse prestin cDNA was translated into a 744-amino acid protein. Using the CLUSTAL method, this protein was aligned with gerbil and rat prestin. This alignment revealed 96–97% amino acid identity among the three rodent species (Fig. 1).

Fig. 2 shows a schematic diagram of prestin. EditSeq analysis of mouse prestin reported an estimated molecular weight of 81.4 kDa and a theoretical isoelectric point of 5.8. Statistical analysis of protein sequences (Brendel et al., 1992) on mouse prestin demonstrated the presence of a positive charge cluster at amino acid positions 557–580 and a negatively charged region at residues 595–614, both of which are located in the carboxy-terminus (Fig. 2). PROSITE analysis (Hofmann et

```
MOUSE   MDHAEENEIPAETQRYYVERPIFSHPVLQERLHVKDKVTESIGDKLKQAFTCTPKKIRNI
GERBIL  MDHAEENEIPVATQKYHVERPIFSHPVLQERLHVKDKVSESIGDKLKQAFTCTPKKIRNI
RAT     MDHAEENEIPAETQKYLVERPIFSHPVLQERLHVKDKVTDSIGDKLKQAFTCTPKKVRNI
        1........10........20........30........40........50.....

MOUSE   IYMFLPITKWLPAYKFKEYVLGDLVSGISTGVLQLPQGLAFAMLAAVPPVFGLYSSFYPV
GERBIL  IYMFLPITKWLPAYKFKEYVLGDLVSGISTGVLQLPQGLAFAMLAAVPPVFGLYSSFYPV
RAT     IYMFLPITKWLPAYKFKEYVLGDLVSGISTGVLQLPQGLAFAMLAAVPPVFGLYSSFYPV
        61......70........80........90........100.......110.....

MOUSE   IMYCFFGTSRHISIGPFAVISLMIGGVAVRLVPDDIVIPGGVNATNGTEARDALRVKVAM
GERBIL  IMYCFFGTSRHISIGPFAVISLMIGGVAVRLVPDDIVIPGGVNATNGTEARDALRVKVAM
RAT     IMYCFFGTSRHISIGPFAVISLMIGGVAVRLVPDDIVIPGGVNATNGTEARDALRVKVAM
        121......130.......140.......150.......160.......170.....

MOUSE   SVTLLSGIIQFCLGVCRFGFVAIYLTEPLVRGFTTAAAVHVFTSMLKYLFGVKTKRYSGI
GERBIL  SVTLLSGIIQFCLGVCRFGFVAIYLTEPLVRGFTTAAAVHVFTSMLKYLFGVKTKRYSGI
RAT     SVTLLSGIIQFCLGVCRFGFVAIYLTEPLVRGFTTAAAVHVFTSMLKYLFGVKTKRYSGI
        181......190.......200.......210.......220.......230.....

MOUSE   FSVVYSTVAVLQNVKNLNVCSLGVGLMVFGLLLGGKEFNERFKEKLPAPIPLEFFAVVMG
GERBIL  FSVVYSTVAVLQNVKNLNVCSLGVGLMVFGLLLGGKEFNERFKEKLPAPIPLEFFAVVMG
RAT     FSVVYSTVAVLQNVKNLNVCSLGVGLMVFGLLLGGKEFNERFKEKLPAPIPLEFFAVVMG
        241......250.......260.......270.......280.......290.....

MOUSE   TGISAGFNLHESYSVDVVGTLPLGLLPPANPDTSLFHLVYVDAIAIAIVGFSVTISMAKT
GERBIL  TGISAGFNLHESYSVDVVGTLPLGLLPPANPDTSLFHLVYVDAIAIAIVGFSVTISMAKT
RAT     TGISAGFNLHESYSVDVVGTLPLGLLPPANPDTSLFHLVYVDAIAIAIVGFSVTISMAKT
        301......310.......320.......330.......340.......350.....

MOUSE   LANKHGYQVDGNQELIALGICNSIGSLFQTFSISCSLSRSLVQEGTGGKTQLAGCLASLM
GERBIL  LANKHGYQVDGNQELIALGICNSIGSLFQTFSISCSLSRSLVQEGTGGKTQLAGCLASLM
RAT     LANKHGYQVDGNQELIALGICNSIGSLFQTFSISCSLSRSLVQEGTGGKTQLAGCLASLM
        361......370.......380.......390.......400.......410.....

MOUSE   ILLVILATGFLFESLPQAVLSAIVIVNLKGMFMQFSDLPFFWRTSKIEPTIWLTTFVSSL
GERBIL  ILLVILATGFLFESLPQAVLSAIVIVNLKGMFMQFSDLPFFWRTSKIELTIWLTTFVSSL
RAT     ILLVILATGFLFESLPQAVLSAIVIVNLKGMFMQFSDLPFFWRTSKIELTIWLTTFVSSL
        421......430.......440.......450.......460.......470.....

MOUSE   FLGLDYGLITAVIIALLTVIYRTQSPSYKVLGQLPDTDVYIDIDAYEEVKEIPGIKIFQI
GERBIL  FLGLDYGLITAVIIALLTVIYRTQSPSYKVLGQLPDTDVYIDIDAYEEVKEIPGIKIFQI
RAT     FLGLDYGLITAVIIALLTVIYRTQSPSYTVLGQLPDTDVYIDIDAYEEVKEIPGIKIFQI
        481......490.......500.......510.......520.......530.....

MOUSE   NAPIYYANSDLYSSALKRKTGVNPALIMGARRKAMRKYAKEVGNANVANATVVKVDAEVD
GERBIL  NAPIYYANSDLYSNALKRKTGVNPALIMGARRKAMRKYAKEVGNANIANAAVVKVDGEVD
RAT     NAPIYYANSDLYSSALKRKTGVNPATIMGARRKAMRKYAKEVGNANIANATVVKVDAEVD
        541......550.......560.......570.......580.......590.....

MOUSE   GENATKPEEEDDEVKFPPIVIKTTFPEELQRFLPQGENVHTVILDFTQVNFVDSVGVKTL
GERBIL  GENATKPEEEDDEVKYPPIVIKTTFPEELQRFMPQTENVHTIILDFTQVNFIDSVGVKTL
RAT     GENATKPEEEDDEVKFPPIVIKTTFPEELQRFLPQGENIHTVILDFTQVNFMDSVGVKTL
        601......610.......620.......630.......640.......650.....

MOUSE   AGIVKEYGDVGIYVYLAGCSPQVVNDLTRNNFFENPALKELLFHSIHDAVLGSQVREAMA
GERBIL  AVMVKEYGDVGIYVYLAGCSPQVVNDLTRNRFFENPALKELLFHSIHDAVLGSHVREAMA
RAT     AGIVKEYGDVGIYVYLAGCSAQVVNDLTSNRFFENPALKELLFHSIHDAVLGSQVREAMA
        661......670.......680.......690.......700.......710.....

MOUSE   EQEATASLPQEDMEPNATPTTPEA
GERBIL  EQEASAPPPQDDMEPNATPTTPEA
RAT     EQETTVLPPQEDMEPNATPTTPEA
        721......730......740..
```
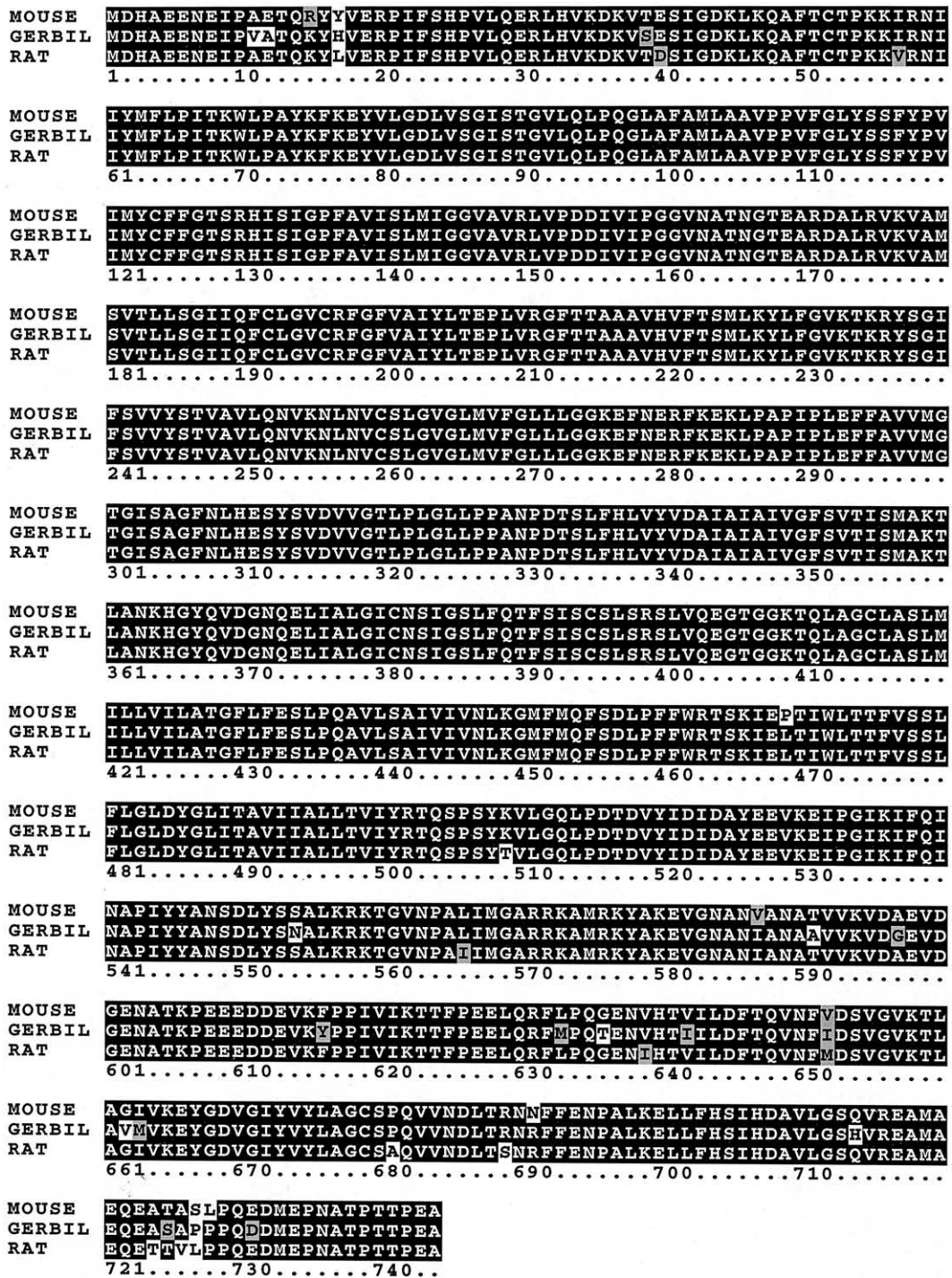
Fig. 1. Alignment of mouse, gerbil, and rat prestin protein sequences. The CLUSTAL program was used to align the three rodent prestin orthologs. This alignment reveals 96–97% identity among the three rodent species. Black and gray regions indicate sequence identity and similarity, respectively. Amino acid positions are denoted by numbers.

al., 1999) of mouse prestin suggested two putative cAMP- and cGMP-dependent protein kinase phosphorylation sites at residues 235–238 (KRYS) and 557–560 (KRKT) as well as one potential tyrosine kinase phosphorylation site at amino acids 665–673. Furthermore, PROSITE analysis revealed four possible *N*-glycosyla-

tion sites at residues 163, 166, 589, and 603; however, the sites at positions 163 and 166 were suggested to be conserved (Zheng et al., 2001). Numerous computer modeling analyses such as TMHMM (Sonnhammer et al., 1998), TMPred (Hofmann and Stoffel, 1993), TopPred (Claros and von Heijne, 1994), SMART

(Schultz et al., 1998, 2000), and HMMTOP (Tusnady and Simon, 1998) on mouse prestin predicted 9–12 membrane-spanning domains. Since Ludwig et al. (2001) and Zheng et al. (2001) reported the cytosolic location of both the carboxy- and amino-termini of rodent prestin, there should be an even number of transmembrane domains (10 or 12). To preserve the conserved sites of N-glycosylation on the extracellular side of mouse prestin, this molecule is shown with 12 potential membrane-spanning regions (Fig. 2). PSI-BLAST analysis (Altschul et al., 1997) on mouse prestin suggested that mouse prestin has high homology to members of the sulfate transporter family, which includes pendrin. Moreover, Pfam analysis (Bateman et al., 1999) indicates that mouse prestin residues 193–503, covering from the fourth to the 12th transmembrane domains, have 38% identity and 58% similarity with the sulfate transport motif. All of the characteristics reported here are in good agreement with the findings of several investigators elsewhere (Zheng et al., 2000, 2001; Ludwig et al., 2001).

3.2. Expression of prestin in the mammalian vestibular and auditory periphery revealed by RT-PCR

Fig. 3 shows two agarose gel images, using either rat or mouse tissue, following RT-PCR. In Fig. 3A, a 626-bp (flanked by oligonucleotides Pres7F and 6R) and a 439-bp (Pres13F and 13R) PCR product appeared in both rat organ of Corti and vestibule, while no prod-
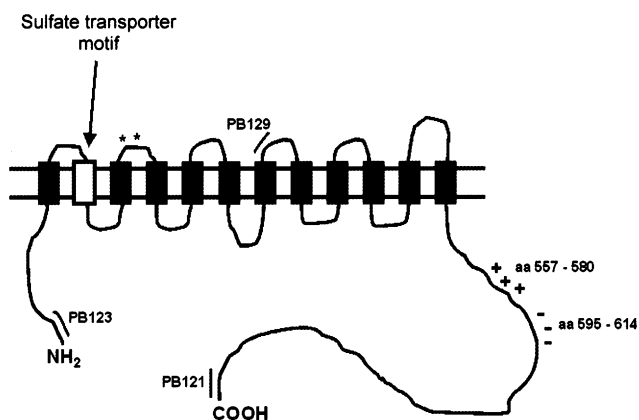
Fig. 2. Schematic diagram of prestin. This protein has 744 amino acids, and depicts 12 membrane-spanning domains, the second of which is a sulfate transporter motif. Both amino- and carboxy-termini are located in the cytosol (Ludwig et al., 2001; Zheng et al., 2001). The carboxy-terminus also exhibits two highly charged regions, one of which is rich in lysine and arginine (aa position 557–580) and the other in aspartic acid and glutamic acid (aa position 595–614). Two conserved sites of N-glycosylation are identified by asterisks at residues 163 and 166. PB121, PB123, and PB129 represent regions against which different antibodies were generated for the purpose of immunolabeling.
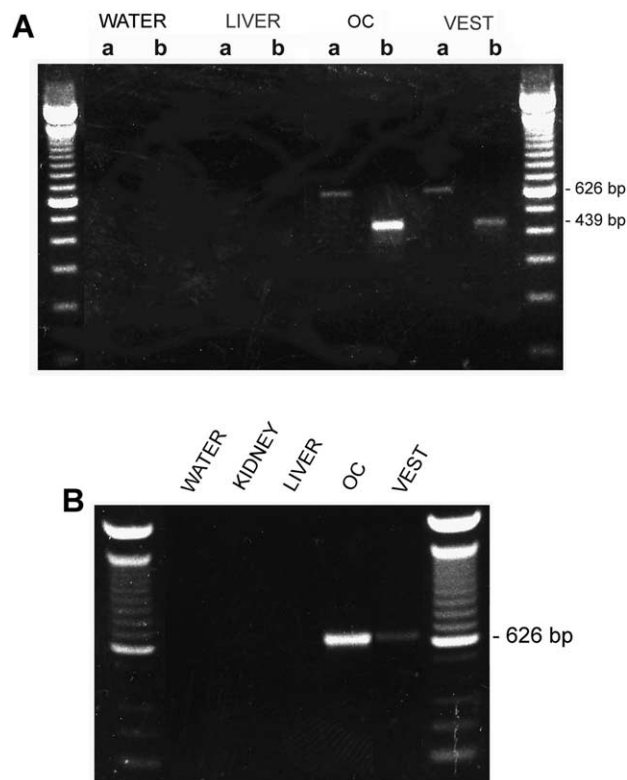
Fig. 3. Agarose gel electrophoresis of PCR products amplified from rat (A) and mouse (B) organ of Corti, vestibule, liver and/or kidney with two pairs of primers (a, Pres7F and Pres6R; b, Pres13F and Pres13R). (A) Rat – both organ of Corti and vestibule express two single bands at 626 bp and 439 bp, while neither water nor rat liver yields any bands. The two bands were sequenced and were shown to be 90–92% identical to similar regions of gerbil prestin cDNA (GenBank accession number AF230376). (B) Mouse – both organ of Corti and vestibule depict a single band at 626 bp (flanked by Pres7F and Pres6R) whose sequence was 92% identical to a similar region of gerbil prestin cDNA. Neither mouse kidney, liver, nor water expresses any bands.

ucts appeared in the control (water) or with rat liver cDNA. The two products were sequenced and, following BLAST searches, revealed 90–92% identity to similar regions of gerbil prestin cDNA. It should be noted that prior to PCR, the RNA concentration of rat vestibule (320 ng/µl) was about 11 times greater than that of rat organ of Corti (30 ng/µl).

Mouse organ of Corti and vestibule expressed single bands flanked by Pres7F and 6R at the length of 626 bp, whereas no band was exhibited in either water, mouse liver, or mouse kidney (Fig. 3B). The 439-bp band using Pres13F and 13R was observed in both organ of Corti and vestibule (data not shown). BLAST searches on these two PCR products yielded 88–92% identity to similar DNA regions of gerbil prestin. In addition, the 626-bp (Fig. 3B) and 439-bp bands (data not shown) appeared more prominent in the organ of Corti than in vestibule.
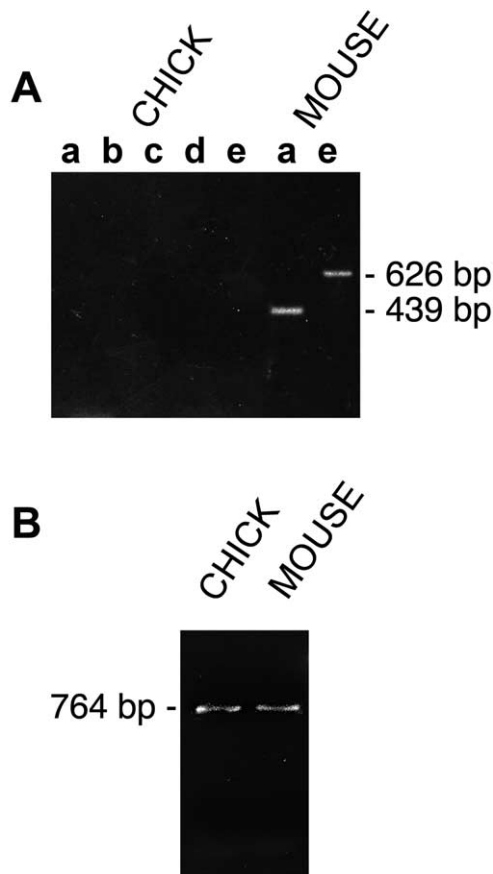
Fig. 4. (A) Agarose gel electrophoresis of PCR products amplified from chicken basilar papilla with five pairs of prestin primers, including Pres13F and 13R (column a) and Pres7F and 6R (e). In addition to the expected lengths of 439 bp (a) and 626 bp (e), PCR with three other pairs of oligonucleotides was expected to yield bands of 414 bp (Pres14F and 14R [b], which flank nucleotides 422–835 of prestin ORF), 371 bp (Pres15F and 15R [c] – nucleotides 1357–1727), and 440 bp (Pres16F and 16R [d] – nucleotides 1676–2115). Chicken basilar papilla lanes do not display any band, while mouse organ of Corti demonstrates a single band flanked by a different pair of oligonucleotides (626 bp sandwiched by Pres7F and 6R; 439 bp flanked by Pres13F and 13R). (B) Agarose gel electrophoresis of PCR products amplified from chicken basilar papilla and mouse organ of Corti with a pair of β-actin amplimers (Clontech Laboratories, Palo Alto, CA, USA). Both chicken and mouse lanes exhibit single bands at 764 bp, the expected length of the β-actin DNA region flanked by these amplimers. The presence of these bands confirms the integrity of the RNA isolated from either rodent or avian ear.

3.3. Prestin was not detected in chicken basilar papilla

Fig. 4A depicts RT-PCR results on chicken basilar papilla cDNA with five different pairs of primers, including the two pairs used for RT-PCR on rat and mouse. The other three pairs of primers were used to clone mouse prestin ORF (together, PCR on rodent organ of Corti with the five pairs of primers yielded 2.0 kb or about 90% of prestin ORF). Mouse organ of Corti with two pairs of prestin oligonucleotides

(Pres7F and 6R or Pres13F and 13R) was used as positive control. The agarose gel image with chicken basilar papilla and mouse organ of Corti PCR products displays only two single bands at 439 bp (sandwiched by Pres13F and 13R) and 626 bp (Pres7F and 6R) in the mouse organ of Corti lanes (Fig. 4A). The lengths of these bands are exactly the same as those of the bands flanked by the same primers in both rat and mouse (Fig. 3). The chicken and mouse ear cDNAs were verified by the presence of a 764-bp band following RT-PCR with β-actin amplimers (Fig. 4B). These data suggest that the chicken basilar papilla PCR products failed to exhibit any bands that would indicate the presence of prestin in the chicken inner ear. This finding confirms and extends the preliminary observations of He et al. (2001).

In a separate set of experiments, we used antibodies against C- and N-termini of gerbil prestin to stain whole-mount preparations of the chicken basilar papilla. No labeling was observed (data not shown).

3.4. Localization of prestin in the mammalian auditory and vestibular periphery

In situ hybridization on whole-mount preparations of mouse and rat organs of Corti with the 626-bp antisense riboprobe resulted in a strong hybridization signal in the three rows of OHCs (Fig. 5A). The sense riboprobe revealed no positive labeling in any whole-mount preparations of rodent organ of Corti (data not shown). *In situ* hybridization with shorter (286 bp) riboprobes verified the above observations (data not shown). These data indicate that within the organ of Corti prestin mRNA is exclusively expressed in OHCs, and confirm the findings of Judice et al. (2002).

In situ hybridization with the 626-bp riboprobes was performed on several portions of the rat, mouse, and gerbil vestibular periphery (Fig. 5B–E). Results were similar in these three rodent species. *In situ* hybridization with the antisense probe produced numerous particulate areas of staining at the sensory epithelium level of the cristae ampullares (Fig. 5B), whereas a similar technique with the sense riboprobe exhibited background only (Fig. 5C). Analogous labeling patterns were obtained in the *in situ* hybridization with the 626-bp antisense and sense riboprobes on rodent utricle whole mounts (Fig. 5D,E). The staining was scattered and irregular but localized to the area of the sensory epithelium (Fig. 5B,D). Similar staining with both 626-bp riboprobes was observed at the sensory epithelium level of the saccule (data not shown). However, it was difficult to determine which cells were stained.

Immunocytochemical staining with three different antibodies against prestin was performed on mouse, rat and gerbil organs of Corti as well as on utricle
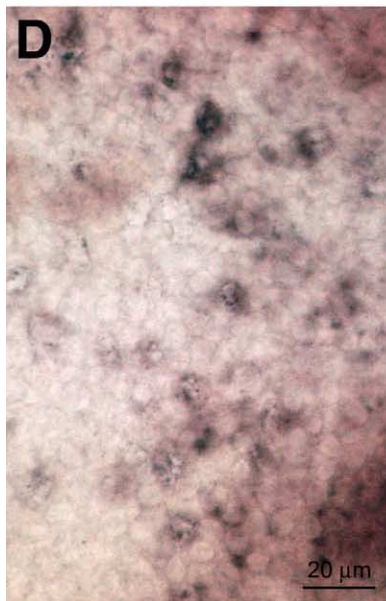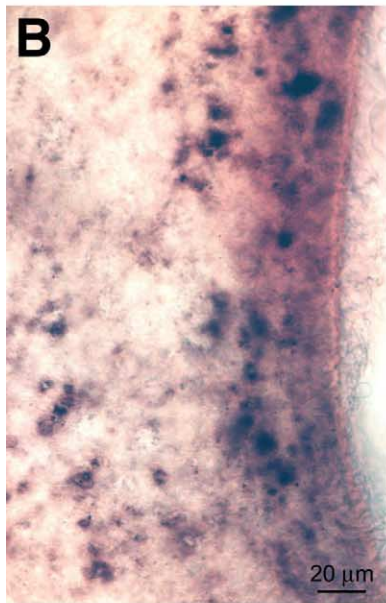
and crista ampullaris tissues. In these species, the labeling in the organ of Corti was restricted to the OHC lateral plasma membrane with all the antibodies (Fig. 6A). In the vestibular periphery, at the focal plane of hair cell nuclei, each antibody stained perinuclear rings of the cytoplasm of some, but not all, cells in the sensory epithelium of the crista ampullaris (Fig. 6B) and the utricle (Fig. 6C). The side view image of VHCs reveals the cytoplasmic distribution of staining (Fig. 6B, inset). The whole mount of crista ampullaris double-stained with rhodamine-phalloidin and N-terminus anti-prestin antibody revealed the labeling in both type I and II hair cells (data not shown). However, the varying levels of the labeling intensity and the scattered pattern of labeling did not allow us to discriminate which type of hair cells was labeled the most.

3.5. VHCs do not possess voltage-dependent capacitance characteristic for OHCs

The expression of prestin in the cell plasma membrane can be tested electrophysiologically by recording the voltage dependence of the cell capacitance. Several cell types with essentially no voltage-dependent capacitance were found to acquire the characteristic bell-shaped voltage dependence of their capacitance after transient transfection with the gene that encodes prestin (Zheng et al., 2000; Santos-Sacchi et al., 2001; Ludwig et al., 2001; Meltzer and Santos-Sacchi, 2001; Santos-Sacchi and Navarrete, 2002). In the whole-cell patch-clamp conditions, we measured the capacitance of isolated type I ($n = 3$) and type II ($n = 4$) VHCs, sweeping the intracellular potential in a broad range of voltages. Fig. 7 shows the comparison of typical capacitance measurements in VHCs and cochlear OHCs. Type I and type II VHCs were identified visually based on the presence of a constricted neck in type I cells and close to cylindrical shape of type II cells (Fig. 7, left insets), as described previously (Wersäll, 1956; Correia et al., 1989). Our measurements showed that the plasma membrane capacitance of both type I and type II VHCs does not depend on the intracellular potential (Fig. 7A,B), in the range of voltages where the capacitance of cochlear OHCs exhibits strong voltage dependence (Fig. 7C). All VHCs tested failed to demonstrate any voltage-dependent changes of the cell capacitance within the accuracy of our experimental technique (< 1 pF, Frolenkov et al., 2000).

4. Discussion

The present paper shows that in the organ of Corti, prestin mRNA is expressed exclusively in OHCs. This finding confirms the localization of prestin in OHCs (Belyantseva et al., 2000; Judice et al., 2002). Mouse prestin has been cloned and characterized, and its comparison with gerbil and rat prestin indicates that the protein is highly conserved among the three rodent species. An important finding of this paper is the expression of prestin in the mammalian vestibular periphery, although such an expression appears to be less prominent than that in the auditory periphery. The observation that the capacitance of VHCs is not voltage-dependent, along with the limited presence of prestin in the rodent utricle, crista ampullaris, and saccule, suggests that the role of prestin in the mammalian vestibular periphery may differ from that in the mammalian auditory periphery. Chicken basilar papilla fails to express prestin, suggesting that prestin may be a characteristic molecule of mammalian hair cells.

4.1. The presence of prestin in the mammalian vestibular periphery

Prestin expression in the mammalian vestibular periphery is an intriguing observation. Our RT-PCR data with different prestin oligonucleotides on mouse and rat vestibular tissues indicated the presence of prestin in these tissues. *In situ* hybridization with prestin riboprobes and immunocytochemistry with three anti-prestin antibodies in three rodent species revealed stained cells in the crista ampullaris and utricle. All these data suggest that prestin is indeed present in the mammalian vestibular periphery.

The fact that prestin and pendrin have some amino acid similarity raises the possibility that the 286-bp and 626-bp probes used for *in situ* hybridization may hybridize with both prestin and pendrin mRNAs. However, this possibility is ruled out, because studies have shown that pendrin mRNA is not expressed in the sensory epithelium of vestibular end-organs (Everett et al., 1999). Even though pendrin knockout mice exhibit abnormal vestibular hair cells, this damage may be a secondary effect of an altered osmotic environment of the endolymph caused by the absence of the anion-transporting function of pendrin (Everett et al., 2001).

Since OHCs and type II VHCs share many common

←

Fig. 5. *In situ* hybridization on whole-mount preparations of rat inner ear sensory epithelium. (A) Organ of Corti whole mount hybridized with 626-bp antisense probe displays intense staining of the three rows of OHCs. (B,D) Whole mounts hybridized with 626-bp antisense probe yield scattered staining of varying intensity in the sensory epithelium of crista ampullaris and utricle, respectively. In B, labeled hair cells were viewed at an angle tangential to the 'saddle' portion of the cristae ampullares. (C,E) Corresponding whole mounts of crista ampullaris and utricle hybridized with 626-bp sense probe demonstrate background only.
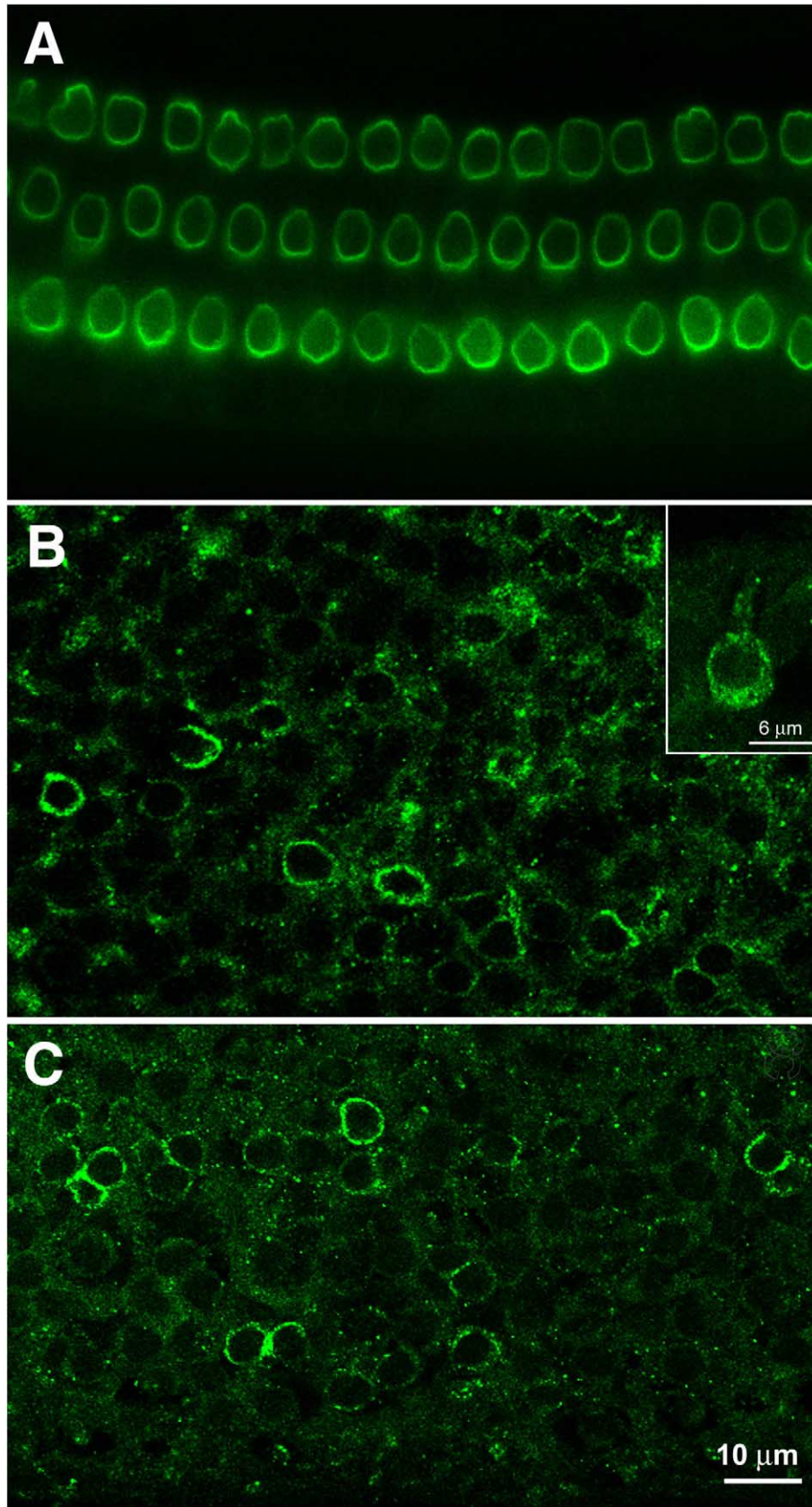
Fig. 6. Immunocytochemical localization of prestin in the mouse organ of Corti and vestibular sensory epithelia with different antibodies (PB121, PB123, PB129). (A) Whole-mount preparation of the organ of Corti labeled with different antibodies. (B) Whole-mount preparation of the crista ampullaris. Inset: Higher resolution image of type I vestibular hair cell. (C) Whole-mount preparation of the utricle.
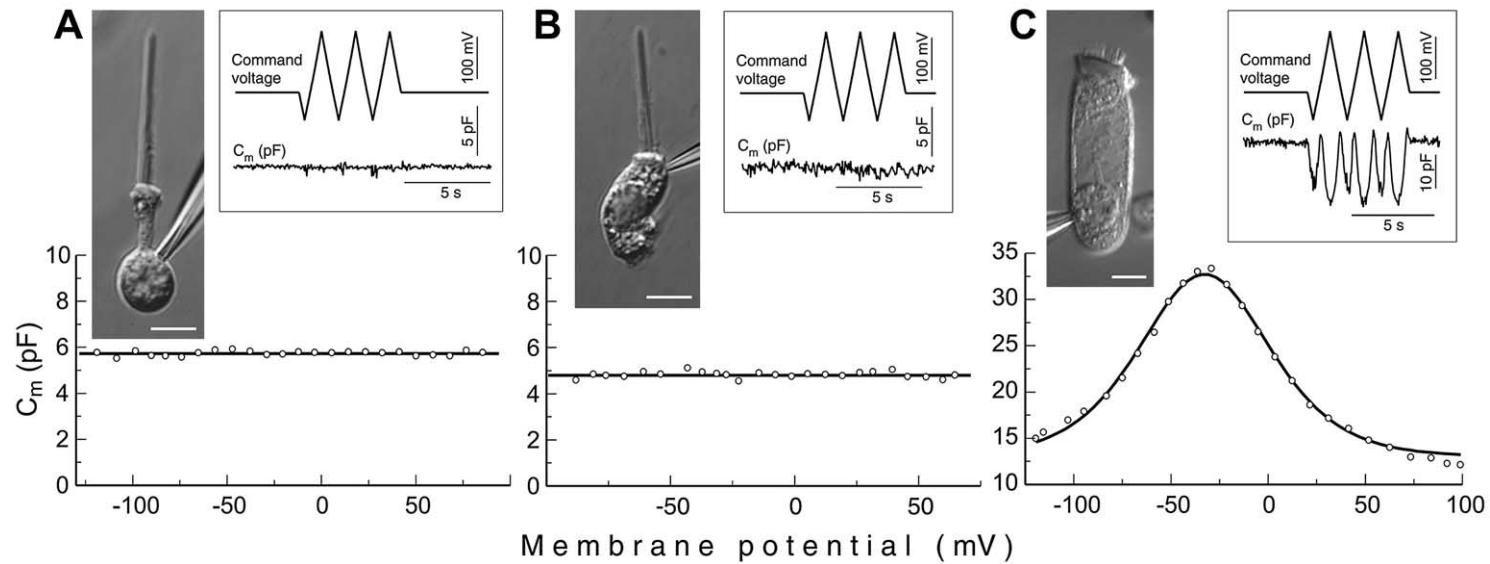
Fig. 7. Voltage dependence of the membrane capacitance of isolated hair cells: VHC type I (A), VHC type II (B), cochlear OHC (C). Left insets show the sample images of the cells. Calibration bars: 5 μm. Right insets show the changes of cell capacitance (lower record) following the application of voltage ramp (upper trace). Open symbols on the graphs represent the capacitance values derived from the data shown in right insets. Data were fitted to the derivative of the Boltzmann function (solid lines). All coefficients of Boltzmann fits for the VHC data (A,B) were statistically non-significant except the values of linear voltage-independent capacitance C_0 (5.73 ± 0.02 pF for VHC type I, 4.82 ± 0.03 pF for VHC type II). Parameters of the fits for the OHC capacitance data in C: $C_0 = 12.7 ± 0.3$ pF, $C_{max} = 20.0 ± 0.3$ pF, $V_p = -32.5 ± 0.5$ mV, $W = 22.6 ± 0.6$ mV. Note that capacitance values for VHCs and OHCs are scaled differently.

characteristics (Eatock et al., 1998; Rusch et al., 1998), it would be tempting to propose that prestin probes and/or antibodies would label type II VHCs. However, variable levels of prestin expression in the vestibule did not allow us to identify which type of hair cell was labeled predominantly, although identification of OHCs in the organ of Corti validated our techniques. Our RT-PCR results also suggest lower levels of prestin expression in vestibule as compared to those in the organ of Corti.

4.2. Prestin was not detected in chicken basilar papilla

To determine the presence of prestin in non-mammalian hair cells, several experiments were carried out on chicken inner ear. Both RT-PCR with prestin oligonucleotides on the chicken basilar papilla and immunocytochemistry with anti-prestin antibodies on the chicken basilar papilla yielded negative results. These data suggest two possible scenarios: either chicken hair cells lack prestin, or these cells may express a homolog of prestin that was not detected by our probes.

4.3. The role of prestin in the mammalian vestibular periphery

As noted in Section 1, prestin has been shown to be localized to the OHC lateral plasma membrane (Belyantseva et al., 2000; Zheng et al., 2000; Ludwig et al., 2001). During inner ear development, the OHC lateral plasma membrane acquires prestin at the same time as electromotility (Belyantseva et al., 2000). When transfected with prestin, cultured cells displayed voltage-dependent membrane length changes (Zheng et al., 2000; Ludwig et al., 2001). Finally, Liberman et al. (2002) demonstrated that prestin knockout mice had elevated threshold sensitivity and that their isolated outer hair cells could not elongate or contract in response to changes in membrane voltage. All these observations suggest that prestin may be primarily responsible for OHC electromotility. Here we demonstrate that prestin is expressed in the cytoplasm of mammalian VHCs, but the function of prestin in the vestibular system remains to be elucidated. Generally, VHCs do not elongate or contract in response to intracellular potential changes, although some active movements of the hair bundle and cuticular plate were observed in type I VHCs (Zenner et al., 1992; Griguer et al., 1993). Here we report that although both type I and type II VHCs seem to have some level of prestin expression, neither of these types of VHCs possesses voltage-dependent capacitance, which would be comparable to that in OHCs. Therefore, it is unlikely that prestin serves the function of 'membrane motor,' as it does in OHCs. However, we cannot exclude the possibility that prestin may be a component of the molecular machinery responsible for the active movements of the hair bundles. It is still possible that prestin is expressed in the plasma membrane of VHCs in very limited amounts, and as a result, it may not be detected by our capacitance measurements and immunofluorescence.

Prestin may be involved in processes other than electromotility. Prestin has high homology to the members of the SLC26 family of anion transport proteins (Dallos and Fakler, 2002) including human pendrin, which is known as a functional chloride-iodide transporter (Scott et al., 1999). Disruption in pendrin induces hearing loss and balance dysfunction (Everett et al., 2001), presumably due to impairment of the ionic equilibrium within the auditory and vestibular periphery (Everett et al., 1999). Apart from being a 'motor' protein in OHCs, prestin may also serve some yet unknown transport function. In fact, the voltage sensitivity of prestin was found to arise from intracellular anions such as chloride and bicarbonate (Oliver et al., 2001). Moreover, recent reports showed that prestin may be involved in sugar transport (Chambard et al., 2003). Our data on the expression of prestin in the vestibular periphery raise again the question about secondary non-motor functions of prestin and establish an important molecular link between auditory and vestibular hair cells.

References

Altschul, S.F., Madden, T.L., Schäffer, A.A., Zhang, J., Zhang, Z., Miller, W., Lipman, D.J., 1997. Gapped BLAST and PSI-BLAST: a new generation of protein database search programs. Nucleic Acids Res. 25, 3389–3402.

Ashmore, J.F., 1987. A fast motile response in guinea-pig outer hair cells: the cellular basis of the cochlear amplifier. J. Physiol. 388, 323–347.

Bateman, A., Birney, E., Durbin, R., Eddy, S.R., Finn, R.D., Sonnhammer, E.L.L., 1999. Pfam 3.1: 1313 multiple alignments match the majority of proteins. Nucleic Acids Res. 27, 260–262.

Belyantseva, I.A., Adler, H.J., Curi, R., Frolenkov, G.I., Kachar, B., 2000. Expression and localization of prestin and the sugar transporter GLUT-5 during development of electromotility in cochlear outer hair cells. J. Neurosci. 20, RC116.

Benser, M.E., Marquis, R.E., Hudspeth, A.J., 1996. Rapid, active hair bundle movements in hair cells from the bullfrog's sacculus. J. Neurosci. 16, 5629–5643.

Beyer, L.A., Qdeh, H., Probst, F.J., Lambert, E.H., Dolan, D.F., Camper, S.A., Kohrman, D.C., Raphael, Y., 2000. Hair cells in

the inner ear of the pirouette and shaker 2 mutant mice. J. Neurocytol. 29, 227–240.

Braissant, O., Wahli, W., 1998a. Differential expression of peroxisome proliferator-activated receptor-alpha, -beta, and -gamma during rat embryonic development. Endocrinology 139, 2748–2754.

Braissant, O., Wahli, W.A., 1998b. Simplified in situ hybridization protocol using non-radioactively labeled probes to detect abundant and rare mRNAs on tissue sections. Biochemica 1, 10–16.

Brendel, V., Bucher, P., Nourbakhsh, I.R., Blaisdell, B.E., Karlin, S., 1992. Methods and algorithms for statistical analysis of protein sequences. Proc. Natl. Acad. Sci. USA 89, 2002–2006.

Brownell, W.E., Bader, C.R., Bertrand, D., de Ribaupierre, Y., 1985. Evoked mechanical responses of isolated cochlear outer hair cells. Science 227, 194–196.

Chambard, J.-M., Harding, I., Ashmore, J.F., 2003. What prestin transports. Abstr. Assoc. Res. Otolaryngol. 26, 104.

Claros, M.G., von Heijne, G., 1994. TopPred II: an improved software for membrane protein structure predictions. Comput. Appl. Biosci. 10, 685–686.

Correia, M.J., Christensen, B.N., Moore, L.E., Lang, D.G., 1989. Studies of solitary semicircular canal hair cells in the adult pigeon. I. Frequency- and time-domain analysis of active and passive membrane properties. J. Neurophysiol. 62, 924–945.

Crawford, A.C., Fettiplace, R., 1985. The mechanical properties of ciliary bundles of turtle cochlear hair cells. J. Physiol. 364, 359–379.

Dallos, P., Evans, B.N., 1995. High-frequency motility of outer hair cells and the cochlear amplifier. Science 267, 2006–2009.

Dallos, P., Fakler, B., 2002. Prestin, a new type of motor protein. Nat. Rev. Mol. Cell Biol. 3, 104–111.

Denk, W., Webb, W.W., 1992. Forward and reverse transduction at the limit of sensitivity studied by correlating electrical and mechanical fluctuations in frog saccular hair cells. Hear. Res. 60, 89–102.

Eatock, R.A., Rusch, A., Lysakowski, A., Saeki, M., 1998. Hair cells in mammalian utricles. Otolaryngol. Head Neck Surg. 119, 172–181.

Everett, L.A., Morsli, H., Wu, D.K., Green, E.D., 1999. Expression pattern of the mouse ortholog of the Pendred's syndrome gene (*Pds*) suggests a key role for pendrin in the inner ear. Proc. Natl. Acad. Sci. USA 96, 9727–9732.

Everett, L.A., Belyantseva, I.A., Noben-Trauth, K., Cantos, R., Chen, A., Thakkar, S.I., Hoogstraten-Miller, S.L., Kachar, B., Wu, D.K., Green, E.D., 2001. Targeted disruption of mouse *Pds* provides insight about the inner-ear defects encountered in Pendred syndrome. Hum. Mol. Genet. 10, 153–161.

Frolenkov, G.I., Atzori, M., Kalinec, F., Mammano, F., Kachar, B., 1998. The membrane-based mechanism of cell motility in cochlear outer hair cells. Mol. Biol. Cell 9, 1961–1968.

Frolenkov, G.I., Mammano, F., Belyantseva, I.A., Coling, D., Kachar, B., 2000. Two distinct Ca^{2+}-dependent signaling pathways regulate the motor output of cochlear outer hair cells. J. Neurosci. 20, 5940–5948.

Gale, J.E., Ashmore, J.F., 1997. An intrinsic frequency limit to the cochlear amplifier. Nature 389, 63–66.

Griguer, C., Lehouelleur, J., Valat, J., Sahuquet, A., Sans, A., 1993. Voltage dependent reversible movements of the apex in isolated guinea pig vestibular hair cells. Hear. Res. 67, 110–116.

He, D., Beisel, K.W., Ding, D., Chen, L., Fritzsch, B., Salvi, R.J., 2001. Are chick hair cells motile? Abstr. Assoc. Res. Otolaryngol. 24, 159.

Hofmann, K., Stoffel, W., 1993. TMbase – A database of membrane spanning proteins segments. Biol. Chem. Hoppe-Seyler 374, 166.

Hofmann, K., Bucher, P., Falquet, L., Bairoch, A., 1999. The PRO-

SITE database, its status in 1999. Nucleic Acids Res. 27, 215–219.

Judice, T.N., Nelson, N.C., Beisel, C.L., Delimont, D.C., Fritzsch, B., Beisel, K.W., 2002. Cochlear whole mount in situ hybridization: identification of longitudinal and radial gradients. Brain Res. Protocols 9, 65–76.

Kachar, B., Brownell, W.E., Altschuler, R., Fex, J., 1986. Electrokinetic shape changes of cochlear outer hair cells. Nature 322, 365–368.

Kalinec, F., Holley, M.C., Iwasa, K.H., Lim, D.J., Kachar, B., 1992. Membrane-based force generation mechanism in auditory sensory cells. Proc. Natl. Acad. Sci. USA 89, 8671–8675.

Liberman, M.C., Gao, J., He, D.Z.Z., Wu, X., Jia, S., Zuo, J., 2002. Prestin is required for electromotility of the outer hair cell and for the cochlear amplifier. Nature 419, 300–304.

Ludwig, J., Oliver, D., Frank, G., Klocker, N., Gummer, A.W., Fakler, B., 2001. Reciprocal electromechanical properties of rat prestin: the motor molecule from rat outer hair cells. Proc. Natl. Acad. Sci. USA 98, 4178–4183.

Manley, G.A., 2000. Cochlear mechanisms from a phylogenetic viewpoint. Proc. Natl. Acad. Sci. USA 97, 11736–11743.

Manley, G.A., Koppl, C., 1998. Phylogenetic development of the cochlea and its innervation. Curr. Opin. Neurobiol. 8, 468–474.

Manley, G.A., Kirk, D.L., Koppl, C., Yates, G.K., 2001. In vivo evidence for a cochlear amplifier in the hair-cell bundle of lizards. Proc. Natl. Acad. Sci. USA 98, 2826–2831.

Martin, P., Hudspeth, A.J., 1999. Active hair-bundle movements can amplify a hair cell's response to oscillatory mechanical stimuli. Proc. Natl. Acad. Sci. USA 96, 14306–14311.

Meltzer, J., Santos-Sacchi, J., 2001. Temperature dependence of nonlinear capacitance in human embryonic kidney cells transfected with prestin, the outer hair cell motor protein. Neurosci. Lett. 313, 141–144.

Morsli, H., Choo, D., Ryan, A., Johnson, R., Wu, D.K., 1998. Development of the mouse inner ear and origin of its sensory organs. J. Neurosci. 18, 3327–3335.

Oliver, D., He, D.Z., Klocker, N., Ludwig, J., Schulte, U., Waldegger, S., Ruppersberg, J.P., Dallos, P., Fakler, B., 2001. Intracellular anions as the voltage sensor of prestin, the outer hair cell motor protein. Science 292, 2340–2343.

Pickles, J.O., Corey, D.P., 1992. Mechanoelectrical transduction by hair cells. Trends Neurosci. 15, 254–259.

Ricci, A.J., Crawford, A.C., Fettiplace, R., 2000. Active hair bundle motion linked to fast transducer adaptation in auditory hair cells. J. Neurosci. 20, 7131–7142.

Rusch, A., Thurm, U., 1990. Spontaneous and electrically induced movements of ampullary kinocilia and stereovilli. Hear. Res. 48, 247–263.

Rusch, A., Lysakowski, A., Eatock, R.A., 1998. Postnatal development of type I and type II hair cells in the mouse utricle: acquisition of voltage-gated conductances and differentiated morphology. J. Neurosci. 18, 7487–7501.

Santos-Sacchi, J., 1991. Reversible inhibition of voltage-dependent outer hair cell motility and capacitance. J. Neurosci. 11, 3096–3110.

Santos-Sacchi, J., Navarrete, E., 2002. Voltage-dependent changes in specific membrane capacitance caused by prestin, the outer hair cell lateral membrane motor. Pflugers Arch. 444, 99–106.

Santos-Sacchi, J., Shen, W., Zheng, J., Dallos, P., 2001. Effects of membrane potential and tension on prestin, the outer hair cell lateral membrane motor protein. J. Physiol. 531, 661–666.

Schultz, J., Milpetz, F., Bork, P., Ponting, C.P., 1998. SMART, a simple modular architecture research tool: identification of signaling domains. Proc. Natl. Acad. Sci. USA 95, 5857–5864.

Schultz, J., Copley, R.R., Doerks, T., Ponting, C.P., Bork, P., 2000.

SMART: a web-based tool for the study of genetically mobile domains. Nucleic Acids Res. 28, 231–234.

Scott, D.A., Wang, R., Kreman, T.M., Sheffield, V.C., Karniski, L.P., 1999. The Pendred syndrome gene encodes a chloride-iodide transport protein. Nat. Genet. 21, 440–443.

Sonnhammer, E.L., von Heijne, G., Krogh, A., 1998. A hidden Markov model for predicting transmembrane helices in protein sequences. Proc. Int. Conf. Intell. Syst. Mol. Biol. 6, 175–182.

Tusnady, G.E., Simon, I., 1998. Principles governing amino acid composition of integral membrane proteins: application to topology prediction. J. Mol. Biol. 283, 489–506.

Wersäll, J., 1956. Studies on the structure and innervation of the sensory epithelium of the crista ampullaris in the guinea pig. Acta Otolaryngol. 126 (Suppl.), 1–85.

Zenner, H.P., Reuter, G., Hong, S., Zimmermann, U., Gitter, A.H., 1992. Electrically evoked motile responses of mammalian type I vestibular hair cells. J. Vestib. Res. 2, 181–191.

Zheng, J., Shen, W., He, D.Z.Z., Long, K.B., Madison, L.D., Dallos, P., 2000. Prestin is the motor protein of cochlear outer hair cells. Nature 405, 149–155.

Zheng, J., Long, K.B., Shen, W., Madison, L.D., Dallos, P., 2001. Prestin topology: localization of protein epitopes in relation to the plasma membrane. NeuroReport 12, 1929–1935.

Zheng, J., Madison, L.D., Oliver, D., Fakler, B., Dallos, P., 2002a. Prestin, the motor protein of outer hair cells. Audiol. Neurootol. 7, 6–8.

Zheng, J., Long, K.B., Robison, D.E., He, D.Z., Cheng, J., Dallos, P., Madison, L.D., 2002b. Identification of differentially expressed cDNA clones from gerbil cochlear outer hair cells. Audiol. Neurootol. 7, 277–288.